ARTICLE

Primary Processes in the Bacterial Reaction Center Revealed by Femtosecond Broadband Fluorescence Spectroscopy†

Heyuan Liu[a,b‡], Zhanghe Zhen[a‡], Lingfeng Peng[c], Hailong Chen[a,b,c*], Yu-Xiang Weng[a,b,c]

a. The Laboratory of Soft Matter Physics, Beijing National Laboratory for Condensed Matter Physics, Institute of Physics, Chinese Academy of Sciences, Beijing 100190, China
b. School of Physical Science, University of the Chinese Academy of Sciences, Beijing 100049, China
c. Songshan Lake Materials Laboratory, Dongguan 523808, China

(Dated: Received on November 26, 2023; Accepted on December 12, 2023)

To gain a deeper understanding of the highly efficient mechanisms within the photosynthetic bacterial reaction center (BRC), we have employed femtosecond broadband fluorescence spectroscopy to investigate the dynamics of initial photo-induced energy transfer and charge separation in BRC at room temperature. Benefiting from the broadband spectral coverage inherent of this technique, two distinct transient emission species associated with bacteriochlorophylls B and P are directly identified, with Stokes shifts determined to be ~197 and 450 cm^{-1}, respectively. The ultrafast energy transfers from bacteriopheophytin H to B (98 fs) and from B to P (170 fs) are unveiled through fitting the emission dynamics. Notably, the anticipated sub-200 fs lifetime of B emission significantly extends to ~400 fs, suggesting a plausible coupling between the electronic excited state of B and the vibronic states of P, potentially influencing the acceleration of the energy transfer process. These findings should pave the way for understanding the impact of vibronic dynamics on the photo-induced primary processes in the photosynthetic reaction center.

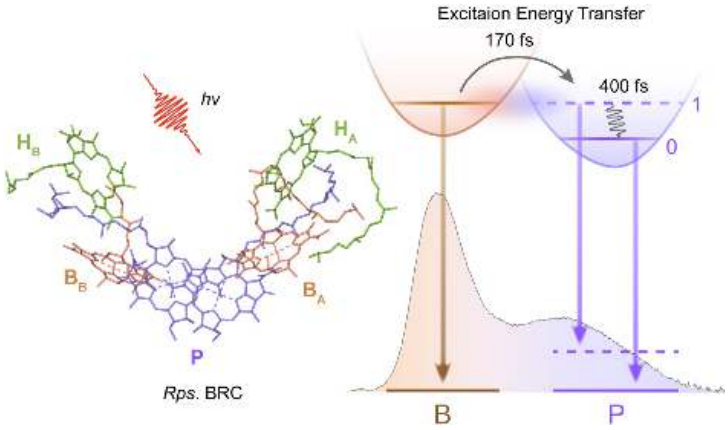

Key words: Bacterial reaction center, Femtosecond broadband fluorescence spectroscopy, Energy transfer, Charge separation, Transient fluorescence

I. INTRODUCTION

The photosynthetic bacterial reaction center (BRC) efficiently converts solar energy into chemical potential energy with near-unity quantum efficiency, making it a crucial model for designing high-conversion artificial light-harvesting systems [1]. This pigment-protein complex consists of three *trans*-membrane polypeptides, namely L, M, and H, encasing ten pigment cofactors organized in two branches with pseudo-twofold symmetry (see FIG. 1(a)) [2–5]. The central pair, known as the "special pair" (P), formed by strongly coupled bacteriochlorophyll-a molecules on the periplasm side, serves

† Part of Special Topic "Ultrafast Spectroscopy focused on Ultrafast Dynamics and Molecular Structures".
‡ These authors contributed equally to this work.
* Author to whom correspondence should be addressed. E-mail: hlchen@iphy.ac.cn

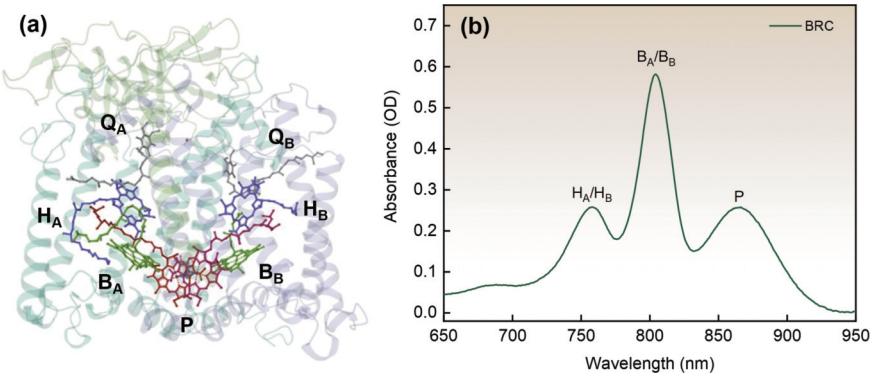

FIG. 1 (a) Structure of the *Rps.* BRC, in which the pigments on A and B branches are labeled. Specifically, P denotes a pair of strongly coupled bacteriochlorophyll-a, B_A and B_B represent bacteriochlorophyll-a, H_A and H_B denote bacteriopheophytin-a, and Q_A and Q_B stand for quinones. (b) The steady-state absorption spectrum of the *Rps.* BRC with the removal of quinones. The absorption bands at 758 nm and 804 nm are attributed to the Q_y electronic transitions of H_A/H_B and B_A/B_B, respectively. The split lower exciton state P_- predominantly contributes to the absorption band at 865 nm, whereas the upper exciton state appears at approximately 814 nm with a smaller oscillator strength.

as the key initiator of primary processes within the BRC. It initiates *trans*-membrane electron transfer to its accessory monomeric bacteriochlorophyll-a (B_A) and bacteriopheophytin-a (H_A) along the functional side, triggering subsequent charge separation events [6–10]. Exciting the special pair P can occur through rapid energy transfer from antenna pigments or direct photon absorption [11, 12]. The initial photo-induced energy transfer and charge separation dynamics of BRC have garnered significant experimental attention over the past three decades.

Martin and Breton pioneered experiments selectively exciting the red absorption region of P using femtosecond transient absorption technique [13]. They determined the charge separation rate of $P^* \rightarrow P^+H_A^- \rightarrow P^+Q_A^-$ to be 2.8 ps and 200 ps. The identification of the intermediate charge separation state $P^+B_A^-$ has provoked debate due to challenges in resolving its spectral features [14–16]. With the improved temporal resolution and sensitivity, Zinth *et al.* successfully detected the short-lived transient component of $P^+B_A^-$, decaying to $P^+H_A^-$ in 0.9 ps [12]. Brederode *et al.* revealed that excitation of B can prompt charge separation either through energy transfer to P* or direct depopulation to $P^+B_A^-$ [17, 18]. However, disentangling the energy and electron transfer timescales in the transient absorption (TA) spectrum remains challenging due to concurrent ground state bleaching, stimulated emission, and electrochromic band shift [19, 20]. To overcome these challenges, transient fluorescence (TF) technique was employed to directly probe the concerned excited state of specific pigments. Boxer's group, for example, conducted femtosecond up-conversion fluorescence measurements, comparing the rising edge of fluorescence from P* through selective excitation of different chromophores, quantitatively extracting energy transfer rates between pigments [21]. However, due to limitations posed by the narrow-band phase-matching condition of the up-conversion method, simultaneous measurement of the TF spectra of the entire BRC complex after photoexcitation remains unattainable. Consequently, a need persists for broadband TF spectral collection of the BRC with femtosecond time resolution to foster a deeper understanding of the high quantum efficiency mechanisms within BRC.

This work utilized the fluorescence non-collinear optical parametric amplification (FNOPA) spectrometer to explore the initial photo-induced energy transfer and charge separation dynamics within the BRC at room temperature. Leveraging the state-of-the-art FNOPA technique, we concurrently gathered broadband TF spectra covering the entire emission spectra of B and P in the BRC, achieving a sub-100 fs time resolution. This approach facilitated the direct identification of transient emission species associated with bacteriochlorophylls B and P and the clear revelation of time constants linked to energy transfer and charge separation dynamics. Additionally, the prolonged lifetime of B emission observed suggests a potential coupling between the electronic excited state of B and the vibronic states of P.

II. MATERIALS AND METHODS

A. Sample preparation

The BRC measured in this work was extracted from

DOI: 10.1063/1674-0068/cjcp2311115

the purple bacteria *Rhodopseudomonas (Rps.) Viridis* and dissolved in a buffer solution. *Rhodopseudomonas spheroids* strain 2.4.1 was grown under semi-anaerobic conditions in light, following previously outlined procedures [22]. The extraction method for BRC was adapted with guidance from Prince *et al.* [23]. Initially, cells were harvested via centrifugation at 5000 g for 10 min, washed, and suspended in 100 mmol/L sodium phosphate (pH 7.4) (buffer A). Subsequently, the cells underwent disruption at 1000 bar using a high-pressure cell crusher (JNBIO JN-2.5, China) followed by centrifugation at 12000 g for 0.5 h to eliminate debris and retrieve the supernatant. Ultracentrifugation at 225000 g for 90 min facilitated the pelleting of chromatophores from the supernatant.

These chromatophores were homogenized in buffer A supplemented with 0.15% dimethyldodecylamine N-oxide (LDAO) (Sigma, USA) and gently stirred at room temperature for 2 h. Subsequently, centrifugation at 225000 g for 60 min at 4 °C was carried out to gather the precipitate, a process repeated once. The resulting precipitate was re-suspended in buffer A containing 1% LDAO and 10 mmol/L Na-ascorbate, stirred in the dark at room temperature for 2 h, and then centrifuged at 25000 g for 120 min to obtain crude BRCs. Overnight dialysis using 20 mmol/L Tris-HCl buffer (pH 8.0) with 0.1% LDAO (buffer B) facilitated further purification.

The subsequent purification involved a 5 mL DEAE column (HiTrap DEAE FF, cytiva, USA), initially washing the column with buffer B and loading the crude BRCs onto it. Following this, a wash with buffer B containing 75 mmol/L NaCl and elution with buffer B containing 200 mmol/L NaCl extracted the BRCs. Additional dialysis with buffer B overnight at 4 °C ensued. Lastly, the BRCs were subjected to cyclic elution on a DEAE column with buffer B containing 4% LDAO and 10 mmol/L *o*-phenanthroline for 6 h to remove quinone, yielding quinone-free BRCs in buffer B containing 200 mmol/L NaCl.

B. Femtosecond TA and broadband TF spectroscopy

The steady-state absorption spectrum was obtained using a custom-built spectrophotometer. For femtosecond TA measurements, the HARPIA-TA spectroscopy system (HARPIA, Light Conversion) was employed. The femtosecond laser (PHAROS, Light conversion) centered at 1030 nm with a pulse repetition rate of 100 kHz and a pulse width of 190 fs drives an optical parametric amplifier (ORPHEUS-HP, Light Conversion), producing tunable pump pulses in the visible range. The pulse energy before the sample was attenuated to 40 nJ. Additionally, a fraction of the 1030 nm laser was focused into a 1 mm thick sapphire crystal, generating supercontinuum white light spanning from 500 nm to 1000 nm as the probe pulses. The relative time delays between the pump and probe pulses were modulated by a mechanical delay stage.

Femtosecond broadband TF measurements were conducted using a custom-built FNOPA spectrometer, previously detailed elsewhere [24–29]. Briefly, the setup involved a Ti:sapphire femtosecond amplifier (Spitfire Ace, Spectra Physics) generating laser pulses centered at 800 nm, with a pulse repetition rate of 5 kHz and a pulse width of 70 fs. A portion of this laser drove an optical parametric amplifier (TOPAS, Spectra Physics) for tunable excitation pulses. Simultaneously, the remaining laser output underwent frequency-doubling to produce a 400 nm laser via a 2 mm thick β-barium borate (BBO) crystal, serving as the FNOPA pump pulses. The energy of the excitation pulses was attenuated to 45 nJ using a neutral density filter. The emitted fluorescence from the BRC sample was collected and focused into a 1 mm thick BBO crystal (cut at $\theta = 32°$, $\alpha = 0°$), and then gated by the 400 nm pump. The amplified fluorescence was gathered using an achromatic lens and coupled into an optical fiber connected to the spectrometer. By adjusting the time delay between the pump and excitation pulses, the femtosecond time-resolved fluorescence can be recorded. The BRC sample was kept stirring in a 1 mm cuvette and underwent measurement in a dark environment to prevent exposure to ambient light.

The TA and TF data were carefully chirp calibrated, and the spectral shape of TF was reconstructed using a previously developed method [30, 31]. All measurements were conducted at room temperature.

III. RESULTS AND DISCUSSION

A. Structure of the pigment-protein complex

The molecular structure of the isolated *Rps.* BRC is illustrated in FIG. 1(a) sourced from PDB file 1AJ [32]. This *trans*-membrane pigment-protein complex comprises three α-helical polypeptide subunits and internal pigment cofactors. Symmetrically arranged polypeptides L and M encase the photosynthetic pigments with-

DOI: 10.1063/1674-0068/cjcp2311115

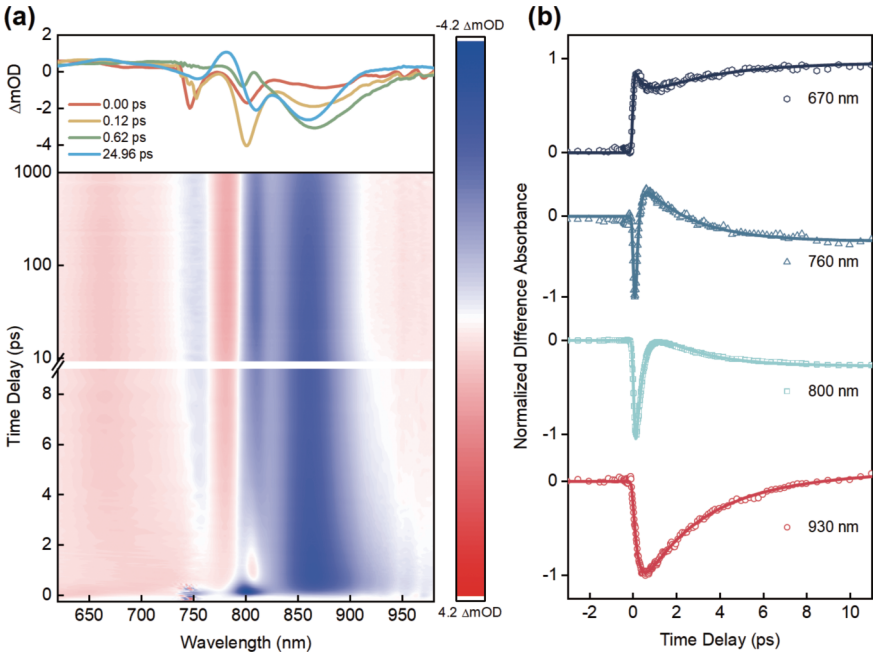

FIG. 2 (a) Lower panel: waiting-time-dependent TA spectra of *Rps.* BRC under 750 nm excitation. Upper panel: spectral slices at four typical waiting times. (b) Temporal evolutions of excitation-induced absorption changes at various wavelengths.

in the BRC, while the H-polypeptide crowns the cytoplasmic facets of L and M. The array of pigment cofactors includes four bacteriochlorophyll-a (BChla), two bacteriopheophytin-a (BPhe), two ubiquinone-10, one carotenoid, and a non-heme iron atom. The "special pair" P, is flanked by two monomeric accessory BChla, designated as B_A and B_B (colored green). The neighboring BPhe and quinones are labeled as H_A and H_B (colored purple), Q_A and Q_B (colored gray). The subscripts A and B correspond to two pigment branches situated on either side of the symmetry axis, with the A-branch typically recognized as the functional branch where electron transfer occurs.

FIG. 1(b) displays the steady-state absorption spectrum of purified *Rps.* BRC in a 1 mm cuvette. Three distinctive peaks observed in the near-infrared region are attributed to the Q_y electronic transitions of BChla and BPhe pigments. The 756 nm band originates from the absorption of two BPhe (H_A, H_B) on each branch, while the 804 nm band is contributed by two BChla (B_A and B_B). Due to the pronounced coupling of the special pair P, the Q_y transition further excitonically splits into higher (P_+) and lower (P_-) states. The split lower exciton state P_- chiefly contributes to the absorption band at 865 nm, while the upper exciton state lies at approximately 814 nm with a smaller oscillator strength [33].

In our experiment, BRC was treated to eliminate Q_A and Q_B, aiming at excluding the long-lived $P^+Q_A^-$ charge-separated state, which decays over the order of 100 ms [34], exceeding the laser repetition interval time.

B. Femtosecond TA measurement

In subsequent femtosecond time-resolved measurements, we selectively excited the BChla (B_A and B_B) and BPhe (H_A and H_B) absorption bands of BRC using 790 nm and 750 nm excitation pulses, respectively. Due to the broad spectral bandwidth of the femtosecond excitation pulses, both branches of pigments (B_A and B_B, as well as H_A and H_B) were concurrently excited. Consequently, for simplicity in the following discussion, we refer to the pigments in BRC collectively as B, H, and P.

We first performed the femtosecond TA measurement. In FIG. 2(a), the waiting-time-dependent TA spectra of *Rps.* BRC under 750 nm excitation are depicted. Here, both H_A and H_B are initially excited, and the results are consistent with prior findings [12, 17, 20, 35]. The upper panel of FIG. 2(a) exhibits TA spectra at various waiting times. Within the initial 200 fs, the sequential emergence of bleaching peaks in the H, B, and P bands was observed. However, due to limitations in the instrumental response function (IRF, ~200 fs) of our TA setup, discerning the discrete energy transfer timescales from H to B and subsequently to P poses a

DOI: 10.1063/1674-0068/cjcp2311115

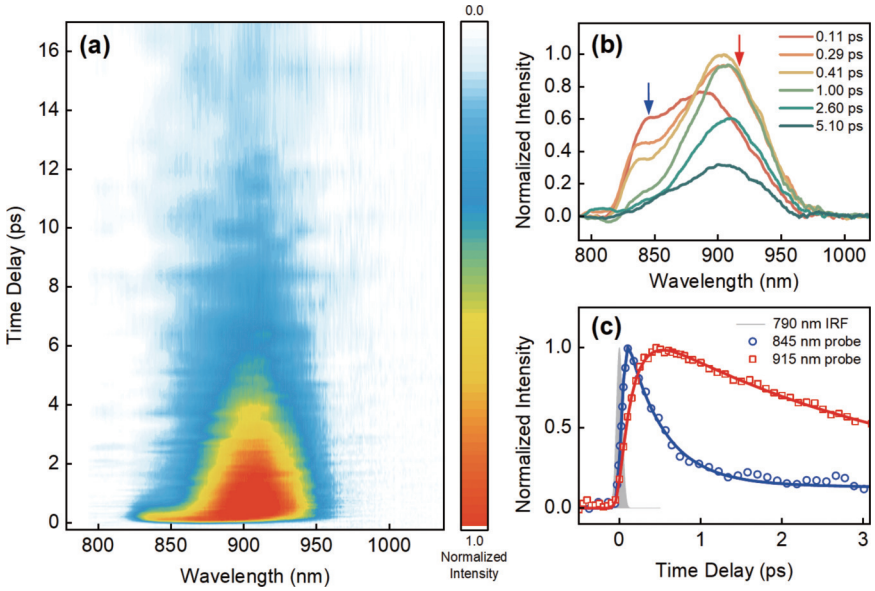

FIG. 3 (a) Waiting-time-dependent TF spectra of *Rps.* BRC under 790 nm excitation. (b) TF spectra at various time delays. The emission at 840 nm and 900 nm arises from the fluorescence transitions of B and P, respectively. (c) TF dynamics probed at 845 nm (blue circles) and 915 nm (red squares). The filled gray curve represents the instrumental response measured using the scattered 790 nm excitation pulse. The dots denote the data points, while the curves denote the multi-exponential fitting, accounting for the IRF (~90 fs).

persistent challenge. Subsequent spectral snapshots at 0.6 ps and 25 ps distinctly display characteristics of charge-separated states $P^+B_A^-$ and $P^+H_A^-$, which were widely reported in the literatures [12, 17, 35].

FIG. 2(b) presents the dynamic traces probed at different wavelengths. The entire TA signals of BRC comprise ground state bleaching, excited state absorption, stimulated emission, and electrochromic band shift induced by charge separation. Consequently, the dynamics at each specific wavelength emerges from a convolution of diverse positive and negative signals originating from multiple sources, significantly challenging further quantitative investigations. Researchers often resort to global fitting methods or employ more intricate techniques like two-dimensional electronic spectroscopy (2DES) to deconvolute the complicated energy transfer and charge separation processes involved in the BRC after the ultrafast photo-excitation [36–39]. These approaches yield distinct kinetic models, contributing to the diversity in understanding these phenomena.

C. Femtosecond TF measurements under selective excitation of H and B

To address the issue mentioned above, femtosecond broadband TF measurements based on the FNOPA technique were conducted. This method inherently resolves the primary processes encompassing energy transfer and charge separation within BRC. FIG. 3(a) illustrates the waiting-time-dependent TF spectra of *Rps.* BRC under 790 nm excitation, initially exciting chromophores B. The fluorescence detection window spans from 800 nm to 1000 nm, allowing for clear delineation of the spectral evolution specific to pigments B and P.

As depicted in FIG. 3(b), two distinct emission species promptly emerge following the photo-excitation, peaking at 840 nm and 900 nm. The emission at 840 nm and 900 nm originates from the fluorescence transitions of B and P, respectively [21, 40–42]. To block the residual 790 nm excitation light, we utilized an 825 nm long-pass filter during the measurement. Consequently, the blue-edge spectral intensity of B emission was significantly reduced. Notably, the fluorescence intensity of B decreases within a few hundred femtoseconds, while that of P initially rises rapidly and then decays within several picoseconds. These observations strongly suggest the occurrence of energy transfer from B to P and subsequent charge separation events.

The corresponding dynamics probed at 845 nm and 915 nm are presented in FIG. 3(c), both can be well-fitted by multi-exponential functions. At 845 nm, the dynamics displays a prominent decaying component of 448±18 fs (depicted as blue circles in FIG. 3(c)), followed by a decay to zero with a time constant of 24±

DOI: 10.1063/1674-0068/cjcp2311115

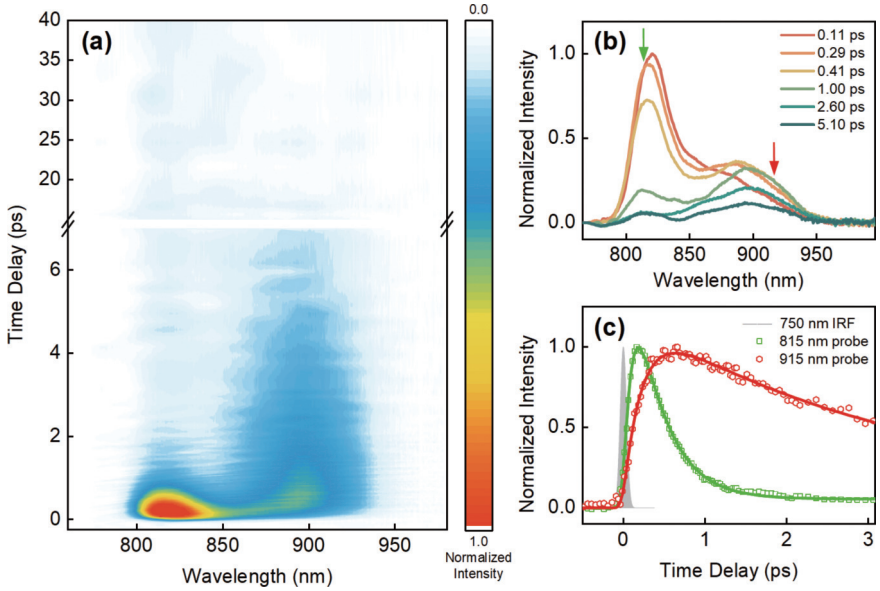

FIG. 4 (a) Waiting-time-dependent TF spectra of *Rps.* BRC under 750 nm excitation. (b) TF spectra at various time delays. The emission at 820 nm and 900 nm arises from the fluorescence transitions of B and P, respectively. (c) TF dynamics probed at 815 nm (green square) and 915 nm (red hexagon). The filled gray curve represents the instrumental response measured using the scattered 750 nm excitation pulse. The dots denote the data points, while the curves denote the multi-exponential fitting, accounting for the IRF (~90 fs).

3 ps. In contrast, the dynamics at 915 nm exhibits a 170±7 fs rise, succeeded by two decaying components of 3.5±0.1 ps and 32.0±5.4 ps.

To further monitor the electronic energy transfer process from H to B, the excitation pulse was adjusted to 750 nm, aligning with the H absorption band. FIG. 4(a) displays the waiting-time-dependent TF spectra of *Rps.* BRC under 750 nm excitation, encompassing the entire emission spectral range of B and P. Here, a high-quality 800 nm long-pass filter with sharp edge of blocking region was utilized to remove the remaining 750 nm excitation light, hindering the direct observation of fluorescence emission from H.

At an earlier waiting time, *e.g.*, 110 fs, distinct spectral features of the B emission become apparent, as depicted in FIG. 4(b). This spectral signature presents an emission species peaking at 820 nm, accompanied by a prolonged tail in the red wing. These characteristics were attributed to the 0-0 transition and higher-order vibronic transitions of BChla, respectively [42–44]. Similar to observations under 790 nm excitation, the 820 nm emission species diminishes while a spectral intensity increase at 900 nm occurs.

Remarkably, the dynamics observed at 815 nm, corresponding to the blue edge of the 0-0 fluorescence transition of B (depicted as green squares in FIG. 4(c)), displays a noticeable rising edge, indicative of the ultrafast energy transfer process from H to B. Considering the IRF (~90 fs), the rise time constant can be fitted as 98±2 fs. Similar to observations under 790 nm excitation, the B emission exhibits a rapid decay of 364±6 fs. In contrast, the dynamics observed at 915 nm, originating from P emission, exhibits a longer rising time constant of 218±9 fs compared to the B band excitation. This emission then rapidly decays with a time constant of 3.1±0.1 ps. Both kinds of dynamics at 815 nm and 915 nm exhibit long-lived components, persisting for at least tens of picoseconds.

D. Photo-induced energy transfer and charge separation dynamics in BRC

Through femtosecond time-resolved broadband TF measurements, the primary processes in BRC after photo-excitation become directly accessible for analysis. Irrespective of excitation to either B or H absorption bands, two primary emission species emerge. The initial appearance of the high-energy species, centered at 820 nm during early waiting times, mirrors the spectral characteristics of BChla, representing the fluorescence of B. In the meanwhile, the major contribution to the red-shifted species after photo-excitation stems from P emission, which is centered at 900 nm. Consequently, the rapid spectral shift between these species signifies an ultrafast energy transfer process from B to P. By

DOI: 10.1063/1674-0068/cjcp2311115

meticulously fitting the rise time of the dynamics at 915 nm, the energy transfer rate from adjacent chromophores to P is directly derived, yielding time constants of 170 fs and 218 fs when selectively exciting B and H, respectively. These findings align with prior reports using femtosecond fluorescence up-conversion spectroscopy to study energy transfer pathways in *Rps.* BRC at 85 K [21]. However, the up-conversion method in previous studies limited detailed experimental observation of TF spectra from B and H emissions. Leveraging our broadband TF spectroscopy (see FIG. 4(a) and (b)), the emission Stokes shifts relative to the absorption peak positions of B and P are precisely obtained as ~197 and 450 cm^{-1}, respectively.

When exciting the B absorption band with 790 nm, an energy flow from B to P contributes to the observed 170 fs rising component. Considering the inter-pigment distances in BRC, initial excitation of the H chromophore at 750 nm leads to an indirect sequential energy transfer from H to B and subsequently to P, contributing to the 218 fs component. Previous research utilizing 2DES with high temporal resolution supported the energy transfer from H to B within both branches of the BRC in sub-100 fs [38]. By fitting the rising dynamics of emission from B under 750 nm excitation (see FIG. 4(c)), the time constant for the energy transfer from H to B, approximately 100 fs, can be directly derived.

In addition, for free BChla molecules in solution, fluorescence lifetimes usually range from hundreds of picoseconds to nanoseconds. In contrast, the emission from excited special pair P in BRC diminishes within several picoseconds due to its preferential relaxation through a charge separation pathway rather than direct relaxation back to the ground state. Consequently, the observed lifetime (~3.5 ps) for the P emission dynamics originates from the photo-induced charge separation process, typically occurring in two sequential steps from P to $P^+H_A^-$ through the $P^+B_A^-$ intermediate [12, 17, 35, 45].

It is worth noting that a rapid decay process of approximately 400 fs is observed in the B emission dynamics upon either excitation of B or H. However, the fitting of the rising edge of P emission dynamics does not reveal any 400 fs component, indicating that this process does not arise from energy transfer between B and P pigments. Although P_+ was initially considered as an intermediate in $B \rightarrow P_-$ transfer, 2DES experiments have revealed an extremely rapid internal conversion from P_+ to P_- with only a 25-fs time constant [38]. Hence, the observed ~400 fs lifetime of B emission cannot be attributed to the presence of the P_+ state. Some previous reports suggested that upon photo-excitation, a portion of B might directly participate in the charge separation process [18, 35]. In such a scenario, the fluorescence dynamics of B should exhibit two independent time constants, corresponding to the energy transfer from B to P and the pathway of charge separation. However, our experimental results demonstrate that the B emission dynamics cannot be fitted to yield a fast component of 100 fs. Fleming *et al.* proposed that the observed 400 fs process in femtosecond TA measurement might stem from the vibrational relaxation of the B ground state [46]. Different from them, our femtosecond TF measurement directly tracks the relaxation process of the B excited state, thereby dismissing the possibility of ground-state vibrational relaxation.

It was revealed that the absorption spectrum of BChla exhibits higher vibronic sidebands [44], marked by structured shoulders on the high-energy side of the main absorption peak. These sidebands cause an overlap between the 0-0 transition absorption peak of B and the 0-1 transition absorption region of P, indicating substantial electron-vibrational coupling between them. Therefore, potential electronic energy transfer pathways within BRC are here proposed (see FIG. 5), which can align well with our experimental TF observations. Specifically, we propose that during the energy transfer from B to P, the vibronic states of P rapidly populate within 200 fs, followed by the charge separation process. Consequently, the P emission dynamics shows a 170 fs rise and a 3.5 ps decay component. Vibrational relaxation of the P vibronic states can endure several hundred femtoseconds. Therefore, the lifetime of B emission significantly extends to ~400 fs due to vibronic mixing or bidirectional energy transfer between the electronic excited state of B and the vibronic states of P. Previous 2DES measurements have highlighted the essential role of pigment vibrational modes in BRC's primary processes, uncovering the presence of vibronic coherence transfer among these pigments [36, 39]. This underscores the plausibility of the vibronically driven energy transfer model as shown in FIG. 5.

We now compare the determined time constants for energy transfer and charge separation in the BRC using TF measurements with those derived from TA dynam-

DOI: 10.1063/1674-0068/cjcp2311115

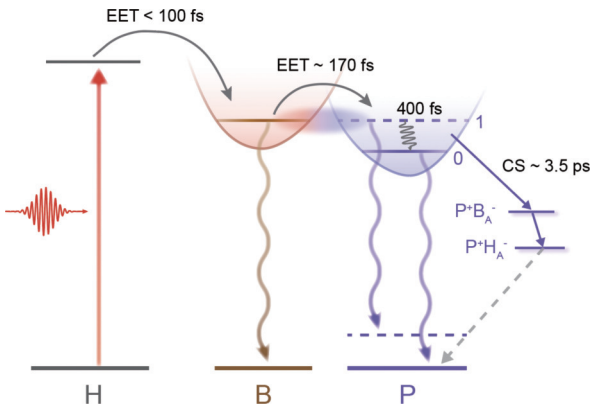

FIG. 5 Scheme of the electronic energy transfer (EET) and charge separation (CS) processes in *Rps.* BRC after the photo-excitation of H. The fluorescence emitted from B and P is depicted as the brown and purple curved arrows, respectively. The vibronic state of P might exert a critical role in the rapid energy transfer from B to P.

ics, illustrated in FIG. 2(b). For example, the rapid decay observed in the TA measurement of the H band's bleaching signal at 760 nm with a time constant of 140±4 fs corresponds to the energy transfer from H to B. However, the limited time resolution of the TA setup (~200 fs) caused an elongation of the bleaching time constant for the H band. The TA measurement fitted a decay time constant of 340±7 fs for the bleaching signal of the B band at 800 nm, while TF analysis revealed a B emission lifetime of ~400 fs, attributed to vibronic mixing. This discrepancy arises because the bleaching signal in TA primarily captures population changes in the electronic ground state, whereas TF directly tracks relaxation processes in the electronic excited state. Furthermore, both the TA measurement of stimulated emission signal at 930 nm and TF measurements directly from P emission exhibit a time constant of ~3.5 ps, indicating involvement in the photo-induced charge separation process.

Lastly, another intriguing observation arises from the TF measurements. Remarkably, even after the completion of charge separation, the fluorescence of BRC still persists, indicating a component with a longer lifetime extending for several tens of picoseconds. Recent investigation highlighted that the involvement of protein dynamics during the initial energy and electron transfer processes might be crucial for this enduring emission component [47]. Nevertheless, unraveling a comprehensive understanding of its underlying physical mechanisms requires more detailed investigation in future studies.

IV. CONCLUSION

In summary, by using state-of-the-art FNOPA spectroscopy, we unveiled the initial photo-induced energy transfer and charge separation dynamics in *Rps.* BRC. Upon photo-excitation of B or H absorption bands, two distinct emission species emerge, which are associated with the fluorescence of B (centered at 820 nm) and P (centered at 900 nm), respectively. TF experimental results indicate the energy transfer time from H to B is less than 100 fs, from B to P is ~170 fs, and the charge separation time is ~3.5 ps. Remarkably, the lifetime of B emission extends significantly to ~400 fs, suggesting a plausible coupling between the electronic excited state of B and the vibronic states of P, potentially influencing the acceleration of the energy transfer process. Further theoretical and experimental exploration is imperative to unveil the intricate role played by vibronic dynamics in photosynthetic energy transfer and charge separation processes.

V. ACKNOWLEDGMENTS

This work was financially supported by the National Key Research and Development Program of China (No.2021YFA1201500), the National Natural Science Foundation of China (No.22027802, No.22222308), the CAS project for Young Scientists and Basic Research (No.YSBR-007), the Natural Science Foundation of Shandong Province (No.ZR2021LLZ003), and the Strategic Priority Research Program of Chinese Academy of Sciences (No.XDB33000000). The authors extend gratitude to Professor Su Lin from Arizona State University, Professor Yueyong Xin from Hangzhou Normal University, and Yarong Shi from the Institute of Physics, Chinese Academy of Sciences, for their invaluable discussions regarding BRC sample preparation.

[1] G. D. Scholes, G. R. Fleming, A. Olaya-Castro, and R. Van Grondelle, Nat. Chem. **3**, 763 (2011).
[2] J. Deisenhofer, O. Epp, K. Miki, R. Huber, and H. Michel, Nature **318**, 618 (1985).
[3] J. Allen, G. Feher, T. Yeates, H. Komiya, and D. Rees, Proc. Natl. Acad. Sci. USA **84**, 5730 (1987).
[4] U. Ermler, G. Fritzsch, S. K. Buchanan, and H. Michel, Structure **2**, 925 (1994).
[5] M. E. van Brederode and M. R. Jones, *Enzyme-Catalyzed Electron and Radical Transfer: Subcellular Bio-*

chemistry, New York: Springer, 621 (2000).
[6] W. W. Parson, Z. T. Chu, and A. Warshel, Biochim. Biophys. Acta **1017**, 251 (1990).
[7] L. M. McDowell, D. Gaul, C. Kirmaier, D. Holten, and C. C. Schenck, Biochemistry **30**, 8315 (1991).
[8] M. Marchi, J. N. Gehlen, D. Chandler, and M. Newton, J. Am. Chem. Soc. **115**, 4178 (1993).
[9] M. A. Steffen, K. Lao, and S. G. Boxer, Science **264**, 810 (1994).
[10] M. Plato, K. Möbius, M. Michel-Beyerle, M. Bixon, and J. Jortner, J. Am. Chem. Soc. **110**, 7279 (1988).
[11] R. van Grondelle, J. P. Dekker, T. Gillbro, and V. Sundstrom, Biochimica et Biophysica Acta **1187**, 1 (1994).
[12] W. Zinth and J. Wachtveitl, ChemPhysChem **6**, 871 (2005).
[13] J. Breton, J.-L. Martin, A. Migus, A. Antonetti, and A. Orszag, Proc. Natl. Acad. Sci. USA **83**, 5121 (1986).
[14] C. Kirmaier and D. Holten, Photosynth. Res. **13**, 225 (1987).
[15] J. S. Joseph, W. Bruno, and W. Bialek, J. Chem. Phys. **95**, 6242 (1991).
[16] J. T. Kennis, A. Y. Shkuropatov, I. H. van Stokkum, P. Gast, A. J. Hoff, V. A. Shuvalov, and T. J. Aartsma, Biochemistry **36**, 16231 (1997).
[17] I. Van Stokkum, L. Beekman, M. Jones, M. Van Brederode, and R. van Grondelle, Biochemistry **36**, 11360 (1997).
[18] M. E. Van Brederode, F. Van Mourik, I. H. Van Stokkum, M. R. Jones, and R. van Grondelle, Proc. Natl. Acad. Sci. USA **96**, 2054 (1999).
[19] S. Lin, A. K. W. Taguchi, and N. W. Woodbury, J. Chem. Phys. **100**, 17067 (1996).
[20] J. Zhu, I. H. van Stokkum, L. Paparelli, M. R. Jones, and M. L. Groot, Biophys. J. **104**, 2493 (2013).
[21] R. J. Stanley, B. King, and S. G. Boxer, J. Chem. Phys. **100**, 12052 (1996).
[22] W. Sistrom, Microbiology **22**, 778 (1960).
[23] R. C. Prince, E. Davidson, C. E. Haith, and F. Daldal, Biochemistry **25**, 5208 (1986).
[24] J. Y. Zhang, C. K. Lee, J. Y. Huang, and C. L. Pan, Opt. Express. **12**, 574 (2004).
[25] P. Fita, Y. Stepanenko, and C. Radzewicz, Appl. Phys. Lett. **86**, 021909 (2005).
[26] X. H. Chen, X. F. Han, Y. X. Weng, and J. Y. Zhang, Appl. Phys. Lett. **89**, 061127 (2006).
[27] X. F. Han, X. H. Chen, Y. X. Weng, and J. Y. Zhang, J. Opt. Soc. Am. B **24**, 1633 (2007).
[28] H. L. Chen, Y. X. Weng, and X. Y. Li, Chin. J. Chem. Phys. **24**, 253 (2011).
[29] P. Mao, Z. Wang, W. Dang, and Y. Weng, Rev. Sci. Instrum. **86**, 123113 (2015).
[30] H. L. Chen, Y. X. Weng, and J. Y. Zhang, J. Opt. Soc. Am. B **26**, 1627 (2009).
[31] W. Dang, Z. Wang, and Y. Weng, Sci. Sin. Chim. **43**, 1713 (2013).
[32] https://www.rcsb.org/3d-view/1AIJ.
[33] M. E. Breton, G. E. Quinn, S. S. Keene, J. C. Dahmen, and A. J. Brucker, Ophthalmology **96**, 1343 (1989).
[34] C. K. Tang, J. C. Williams, A. K. Taguchi, J. P. Allen, and N. W. Woodbury, Biochemistry **38**, 8794 (1999).
[35] M. Du, S. J. Rosenthal, X. Xie, T. J. DiMagno, M. Schmidt, D. K. Hanson, M. Schiffer, J. R. Norris, and G. R. Fleming, Proc. Natl. Acad. Sci. USA **89**, 8517 (1992).
[36] D. Paleček, P. Edlund, S. Westenhoff, and D. Zigmantas, Sci. Adv. **3**, e1603141 (2017).
[37] A. Konar, R. Sechrist, Y. Song, V. R. Policht, P. D. Laible, D. F. Bocian, D. Holten, C. Kirmaier, and J. P. Ogilvie, J. Phys. Chem. Lett. **9**, 5219 (2018).
[38] A. Niedringhaus, V. R. Policht, R. Sechrist, A. Konar, P. D. Laible, D. F. Bocian, D. Holten, C. Kirmaier, and J. P. Ogilvie, Proc. Natl. Acad. Sci. USA **115**, 3563 (2018).
[39] F. Ma, E. Romero, M. R. Jones, V. I. Novoderezhkin, and R. van Grondelle, Nat. Commun. **10**, 933 (2019).
[40] B. A. King, R. J. Stanley, and S. G. Boxer, J. Phys. Chem. B **101**, 3644 (1997).
[41] B. A. King, T. B. McAnaney, A. Dewinter, and S. G. Boxer, J. Phys. Chem. B **104**, 8895 (2000).
[42] X. J. Jordanides, G. D. Scholes, and G. R. Fleming, J. Phys. Chem. B **105**, 1652 (2001).
[43] M. Ratsep, J. Linnanto, and A. Freiberg, J. Chem. Phys. **130**, 194501 (2009).
[44] M. Ratsep, J. M. Linnanto, and A. Freiberg, J. Phys. Chem. B. **123**, 7149 (2019).
[45] M. R. Jones, Biochem. Soc. Trans. **37**, 400 (2009).
[46] Y. Jia, D. M. Jonas, T. Joo, Y. Nagasawa, M. J. Lang, and G. R. Fleming, J. Chem. Phys. **99**, 6263 (1995).
[47] H. Wang, S. Lin, J. P. Allen, J. C. Williams, S. Blankert, C. Laser, and N. W. Woodbury, Science **316**, 747 (2007).

DOI: 10.1063/1674-0068/cjcp2311115